Vol. 91: 67–82, 2023
https://doi.org/10.3354/cr01720

CLIMATE RESEARCH
Clim Res

Published September 21

Contribution to CR Special 36 'Observed changes in climate over Asia'

Asian climate warming since 1901: observation and simulation

Xiubao Sun[1], Guoyu Ren[2,3], Yuyu Ren[3,*], Wei Lin[1], Panfeng Zhang[4], Siqi Zhang[3], Xiaoying Xue[2,3]

[1]State Key Laboratory of Tropical Oceanography, South China Sea Institute of Oceanology, Chinese Academy of Sciences, Guangzhou 510301, PR China

[2]Department of Atmospheric Sciences, School of Environmental Sciences, China University of Geosciences, Wuhan 430074, PR China

[3]Laboratory for Climate Research, National Climate Center, China Meteorological Administration, Beijing 100081, PR China

[4]College of Tourism and Geography, Jilin Normal University, Siping 136000, PR China

ABSTRACT: Land surface air temperature in Asia has been increasing significantly since the 1950s. However, current understanding of Asian warming since 1901 in terms of observations and simulations is still poor. Based on a newly developed observation dataset with 2658 stations and Coupled Model Intercomparison Project Phase 5/6 (CMIP5/6) output data, we analyze changes in mean (T_{mean}), maximum (T_{max}), and minimum (T_{min}) temperature, and diurnal temperature range (DTR) over Asia during 1901–2100. Annual mean land surface air temperature over Asia increased significantly, and T_{mean}, T_{max}, and T_{min} increased by 1.81, 1.47, and 2.15°C during 1901–2020, respectively. The T_{min} warming rate is about 1.5× that of T_{max}, resulting in a decline of Asian DTR by 0.68°C since 1901. We also found that Asia has experienced more substantial warming than the global case and the Northern Hemisphere, and the decline in DTR is more substantial in Asia. Spatially, Asia exhibits a general warming trend with a gradual increase in spatial warming from low to high latitudes, and the effect of high-latitude warming has gradually strengthened since the 2000s. Seasonally, Asian warming in the cold season is stronger than in the warm season. Furthermore, CMIP5/6 can capture the Asian warming in the historical period 1901–2020. However, it underestimated T_{min} and overestimated T_{max}, contributing to their poor performance in simulating the historical change of DTR. Under Shared Socioeconomic Pathway (SSP) 2-4.5, Asian T_{mean}, T_{max}, and T_{min} are projected to increase by 3.5, 3.4, and 3.7°C century^{-1} during 2021–2100, respectively. The Asian warming rate under SSP5-8.5 is about 2× that of SSP2-4.5.

KEY WORDS: Asian warming · Land surface air temperature · Trends · CMIP5/6 · Climate change

1. INTRODUCTION

The Asian continent spans multiple climatic zones, from the equator to the Arctic, resulting in various and complex climate conditions. As home to the largest land area on Earth and in the Northern Hemisphere, Asia experiences more substantial warming rates than the global average (Sun et al. 2017, Xu et al. 2018), and is projected to continue to warm in the future (IPCC 2021). Asian warming has resulted in a drastic change in Asian glaciers, water resources (Alcamo et al. 2007, Piao et al. 2010, Sorg et al. 2012), food security (Saseendran et al. 2000, Piao et al. 2010), and human health (Dhiman et al. 2010). Given the impact of Asian warming on these various aspects over the last century, it is crucial to investigate the spatial and temporal changes in Asian warming since 1901.

Observations show that Asian warming during the last century, particularly after the 1950s, was more substantial than global and other continental warming (Xu et al. 2018, H. M. Zhang et al. 2020, P. F.

*Corresponding author: renyuyu@cma.gov.cn

Publisher: Inter-Research · www.int-res.com

Zhang et al. 2021). Asian warming in the 20th century has also been confirmed by robust observational evidence at regional scales. However, the degree of warming varied significantly across the continent, with distinct seasonal changes and phasic processes.

Some studies have reported more substantial surface warming in East Asia than in the Northern Hemisphere and globally. Multiple observational data show that the mean temperature (T_{mean}) in China has experienced a warming rate of approximately 0.08–0.10°C decade^{-1} from the 1900s to the 2000s (Tang & Ren 2005, Li et al. 2010, Cao et al. 2013). Moreover, China has experienced 2 rapid warming periods: one from 1901 to the 1940s and the other after the 1980s (Ding & Dai 1994, Ding et al. 2007, Yan et al. 2020). Similar T_{mean} changes have also been detected in Japan, South Korea, and the Democratic People's Republic of Korea (Jung et al. 2002, Yue & Hashino 2003, Om et al. 2019). In South Asia, previous studies found that the warming in the 20th century differed in monsoon and post-monsoon seasons. In India, Dash et al. (2007) indicate that T_{mean} increased by 1 and 1.1°C during winter and post-monsoon months in the 20th century, respectively. In Central Asia, observational data from the Goddard Institute for Space Studies (GISS) showed that T_{mean} increased by 0.073°C decade^{-1} from 1880 to 2011. In addition, there was a transition from warm and dry to warm and wet around the 1970s (Shi et al. 2007). Chen et al. (2011) found that the warming rates of T_{mean} in these arid regions are higher than in humid regions, especially in winter. According to observations in the Arctic region, the most significant Arctic warming in the past 400 yr has occurred during the 20th century (Overpeck et al. 1997), and the Arctic's strong warming can even influence global warming trends, especially in winter (Dai et al. 2019). Other high-latitude regions in Asia also experienced strong warming throughout the 20th century (Groisman et al. 2013, Kumar et al. 2014), and Russia's warming even reached 0.39°C decade^{-1} during the period 1972–2006 (Meleshko et al. 2008).

In addition to observations, previous studies have evaluated and projected Asian warming in global coupled models. Fan et al. (2020) indicated that Coupled Model Intercomparison Project (CMIP) Phase 6 (CMIP6) models could capture the interdecadal changes in T_{mean} since the early 20th century on a global scale. According to some previous studies (Jiang et al. 2020, Zhu & Yang 2020, You et al. 2021), lower warming rates and poor interdecadal simulation still exist in CMIP6's simulation of T_{mean} in China since the 1950s, although the climatology simulation performance of the CMIP6 models has been improved from CMIP Phase 5 (CMIP5). Under different emission scenarios within CMIP6, Asian T_{mean} projections show more substantial warming at high latitudes and weaker warming in the tropics and the southern part of the Northern Hemisphere (Fan et al. 2020). In China, T_{mean} is projected to increase by 1.08, 2.97, and 5.62°C, respectively, under Shared Socioeconomic Pathways (SSPs) SSP1-2.6, SSP2-4.5, and SSP5-8.5 in 2081–2100 relative to the current climate period (You et al. 2021). In South Asia, T_{mean} is projected to increase by 1.2, 2.1, and 4.3°C under SSP1-2.6, SSP2-4.5, and SSP5-8.5 by the end of the 21st century, respectively.

Overall, in recent years, there have been some studies on the warming of Asia since the 1950s, but more of them have focused on specific regions or countries. This has resulted in a poor understanding of Asian warming since 1901, especially regarding historical and future changes in T_{mean}, maximum temperature (T_{max}), minimum temperature (T_{min}), and diurnal temperature range (DTR) across Asia. For this study, we reanalyzed the spatiotemporal changes in annual and seasonal T_{mean}, T_{max}, T_{min}, and DTR in Asia since 1901 using the C-LSAT dataset developed by the China Meteorological Administration. We compared them with results from the Climatic Research Unit (CRU) dataset. Additionally, based on CMIP5/6 model output data, we evaluate the performance of the models for Asian warming and project the temperature changes under different SSP scenarios.

2. DATA AND METHODS

2.1. Observational data

Observed T_{mean}, T_{max}, and T_{min} used in this study during 1901–2020 are from the C-LSAT v.1.1 dataset (Sun et al. 2017, Xu et al. 2018) developed by the China Meteorological Administration (CMA), National Meteorological Information Center (http://data.cma.cn/). As described in Sun et al. (2017) and Xu et al. (2014): 'The original data sources of CMA-LSAT data include 3 global datasets (Global Historical Climatology Network-V3 dataset (GHCN-V3), Climatic Research Unit Temperature 4.0 dataset (CRUTEM4.0), and Berkeley Earth Surface Temperature dataset (BEST)); 2 regional datasets (European Climate Assessment & Dataset (ECA&D), and Historical Instrumental Climatological Surface time series of the greater Alpine region database (HISTALP)); and 8

national datasets (China, USA, Russia, Canada, Australia, Korea, Japan, Vietnam).'

Further, the C-LSAT integrated dataset was carried out for quality control and the homogenization process. Quality control mainly refers to the methods used in the GHCN dataset (Menne et al. 2009, Lawrimore et al. 2011). The RHtest-V3 system developed by Wang (2008a,b) is mainly used for the non-homogenized station test. For a more specific introduction to the C-LSAT dataset, please refer to Sun et al. (2017) and Xu et al. (2018).

Sun et al. (2017) have compared the advantages of the C-LSAT and other station datasets. The dataset's station advantages in Asia are primarily concentrated in the surrounding areas of China and high latitudes, with the addition of several unique stations. For example, the dataset includes a collection of 24 stations in China that have a record length of >100 yr.

The study area is Asia, as defined by the World Meteorological Organization (WMO), shown in Fig. 1a as the blue area. We minimized data uncertainties by adopting specific station-selection criteria, which required that stations:

- Have a record length of ≥40 yr in the study period (1901–2020) and an observational record of ≥15 yr in the climate base period (1961–1990).
- Possess ≥9 mo of observation records per year to be considered valid.
- When estimating the trend from 2001 to 2020, the station selected must conform to the above-mentioned criteria, and it is not required to have a record length >10 yr from 2001 to 2020.

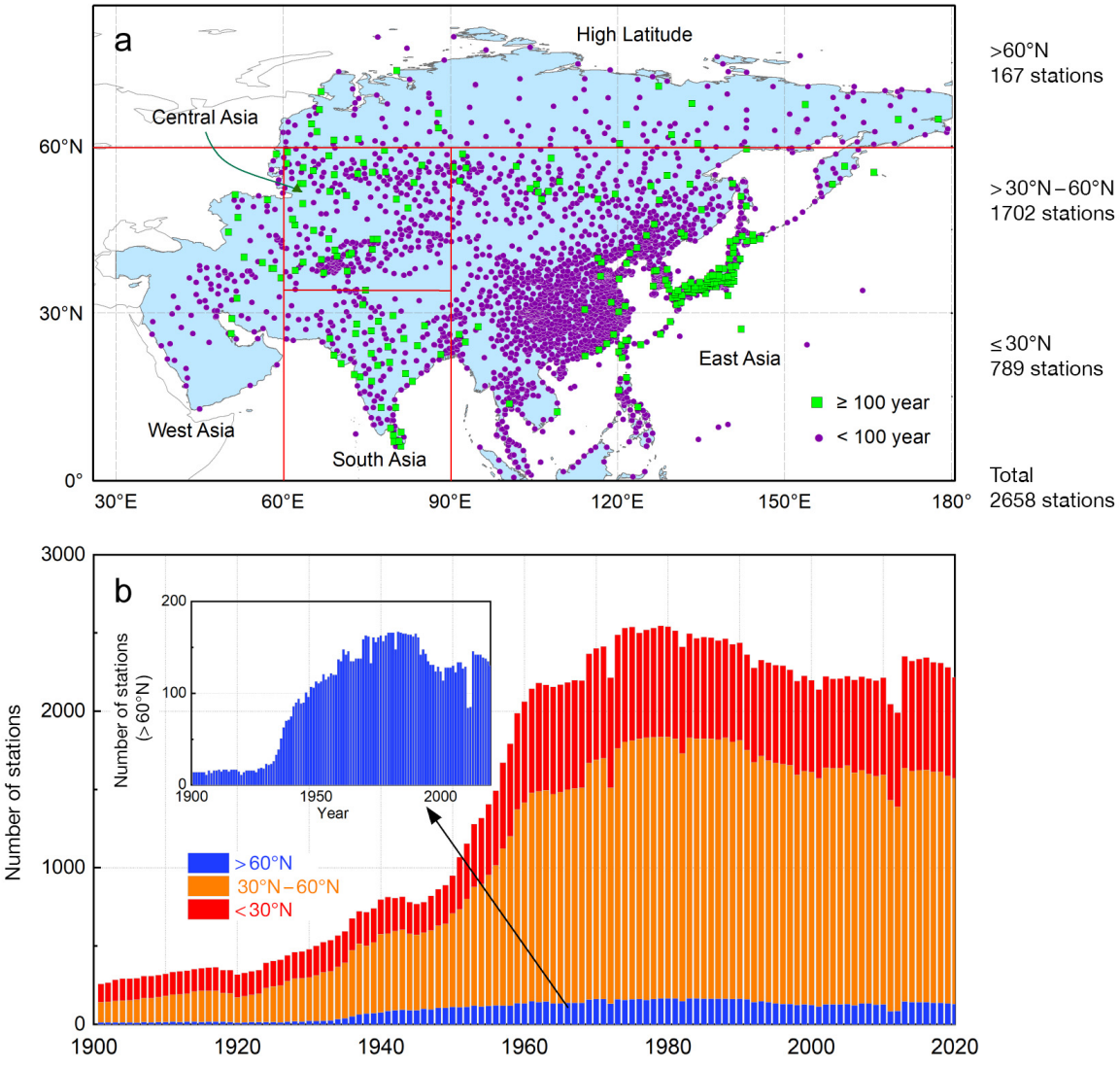

Fig. 1. (a) Observation stations in Asia (to the right of the graph: number of stations at different latitudes). (b) Changes in the number of stations at different latitudes from 1901 to 2020 (inset: only those at >60° N)

The study assessed 2658 stations across Asia that met the selection criteria (shown in Fig. 1a as purple dots and green squares). Stations located >60° N latitude and those in West Asia have poor spatial coverage compared to other areas in Asia, and high spatial coverage is mainly concentrated in China, Japan, and South Korea. Before the 1950s, the number of stations increased from 250 to >1000. Since the 1960s, the number of stations has remained >2000 consistently, as shown in Fig. 1b.

Fig. 1a shows 251 stations with records exceeding 100 yr. Stations with >100 yr of records are mainly distributed in Central and South Asia. In East Asia, most of the stations that meet this criterion can be found in eastern China, Japan, South Korea, and southeastern Russia. Conversely, West Asia and high latitudes have fewer stations with such long records.

In addition, to compare C-LSAT against the most widely used existing dataset in representing Asian and sub-regional warming, we also used T_{max}, T_{min}, and DTR data from the high-resolution CRU TS4.0.4 version dataset, with a spatial data resolution of 0.5° × 0.5° (Harris et al. 2020). Based on C-LSAT and CRU datasets, we compared the warming in Asia and its 5 sub-regions: East Asia (0–60° N, 90–180° E), Central Asia (35–60° N, 60–90° E), West Asia (0–60° N, 35–60° E), South Asia (0–35° N, 60–90° E), and the High Latitudes (60–90° N, 35–180° E). The sub-regions are defined as shown in Fig. 1a.

Table 1. The CMIP5 and CMIP6 models used in this study. Null values: no simulated data. MIP: Model Intercomparison Project

Model no.	Model name	Historical	Scenario MIP
CMIP6			
1	ACCESS-CM2	✓	✓
2	ACCESS-ESM1-5	✓	✓
3	AWI-ESM-1-1-LR	✓	
4	BCC-CSM2-MR	✓	✓
5	BCC-ESM1	✓	
6	CanESM5	✓	✓
7	CMCC-ESM2	✓	✓
8	EC-Earth3	✓	✓
9	EC-Earth3-AerChem	✓	
10	EC-Earth3-CC	✓	✓
11	EC-Earth3-Veg	✓	✓
12	EC-Earth3-Veg-LR	✓	
13	FGOALS-g3	✓	✓
14	FIO-ESM-2-0	✓	✓
15	GISS-E2-1-G	✓	
16	GISS-E2-1-H	✓	
17	INM-CM4-8	✓	✓
18	INM-CM5-0	✓	✓
19	IPSL-CM6A-LR	✓	✓
20	MPI-ESM-1-2-HAM	✓	
21	MPI-ESM1-2-HR	✓	✓
22	MPI-ESM1-2-LR	✓	✓
23	MRI-ESM2-0	✓	✓
	Total	23	16
CMIP5			
1	ACCESS1-3	✓	✓
2	CSIRO-Mk3-6-0	✓	✓
3	GFDL-CM3	✓	✓
4	GFDL-ESM2M	✓	✓
5	GISS-E2-H	✓	✓
6	GISS-E2-R	✓	✓
7	HadGEM2-ES	✓	✓
8	MIROC-ESM	✓	✓
9	MIROC-ESM-CHEM	✓	✓
10	MRI-CGCM3	✓	✓
11	NorESM1-M	✓	✓
	Total	11	11

2.2. CMIP5/6 output data

Model simulations of historical T_{max} and T_{min} data are obtained from 11 models in CMIP5 and 23 models in CMIP6 (Table 1), covering the period 1901–2020. The data used by CMIP5 (CMIP6) for 2006–2020 (2015–2020) is based on SSP2-4.5. Projected T_{max} and T_{min} data are obtained from 16 models in CMIP6 under SSP2-4.5 and SSP5-8.5, covering the period 2021–2100 (Table 1). The spatial resolution of the models varies from 0.5° to 2.5°, and therefore for consistency, all simulations are regridded to the resolution 5° × 5° to match the observations using the bilinear interpolation method.

2.3. Methods

The method for constructing an Asian anomaly time series was as follows. The construction of the time series refers to the area-weighted average method of Jones (1994). First, all stations were divided into a 5 × 5° latitude and longitude grid box (274 in total of 5 × 5° latitude and longitude grid boxes in Asia), with each grid having ≥1 station; then, the anomaly of each grid box value was calculated, and the latitude cosine of the grid center point was used as the weighting coefficient of the area-weighted average, and finally the regional time series was obtained. The Theil-Sen trend estimation method was used to estimate the trend (Sen 1968), and the Mann-Kendall test to test the trend significance level ($p < 0.05$).

3. OBSERVED ASIAN WARMING

3.1. Asian warming during 1901–2020

From 1901 to 2020, T_{mean}, T_{max}, and T_{min} in Asia demonstrated an upward trend (Fig. 2a). Since 1901, the warming of T_{mean}, T_{max}, and T_{min} in Asia can be divided into 3 phases: an early warming period before the 1940s; a period of insignificant change from the 1950s to 1970s; and a rapid warming period after the 1970s. Moreover, Asia also experienced a warming slowdown from the late 1990s to 2014. Additionally, the 10 hottest years for T_{max} and T_{min} since 1901 occurred after 2000, with 2020 ranking as the hottest year.

From 1901 to 2020, Asia's T_{max} and T_{min} show different warming rates, with T_{max} increasing by 1.47°C and T_{min} increasing by 2.15°C. These long-term asymmetric changes reduced DTR by 0.68°C during 1901–2020. Before the 1950s, T_{max} showed more substantial warming than T_{min}, and after the 1950s, T_{min} showed more substantial warming than T_{max}, which led to a trend reversal of DTR from increasing to decreasing around the 1950s (Fig. 2b). This DTR trend reversal phenomenon was also reported globally and for the Northern Hemisphere (Thorne et al. 2016, X. B. Sun et al. 2019).

Fig. 3 illustrates the spatial patterns of the warming trends across Asia. T_{mean}, T_{max}, and T_{min} in Asia consistently show a gradual increase in spatial warming from low to high latitudes, with an overall warming trend observed from 1901 to 2020. From 1961 to 2020, the spatial non-uniformity of Asian warming increased, and the warming became stronger at high latitudes, where T_{min} warming is more substantial than T_{max}. From 2001 to 2020, the spatial non-uniformity of Asian warming increases further, and the middle and low latitudes do not show more substantial warming than other periods, while the warming at high latitudes almost dominates the Asian warming in this period. Additionally, the long-term trends since 1901 and since 1961 reveal a broad decline in DTR, while the decline in DTR after 2001 was concentrated mainly in East Asia, with other Asian regions showing non-uniform changes.

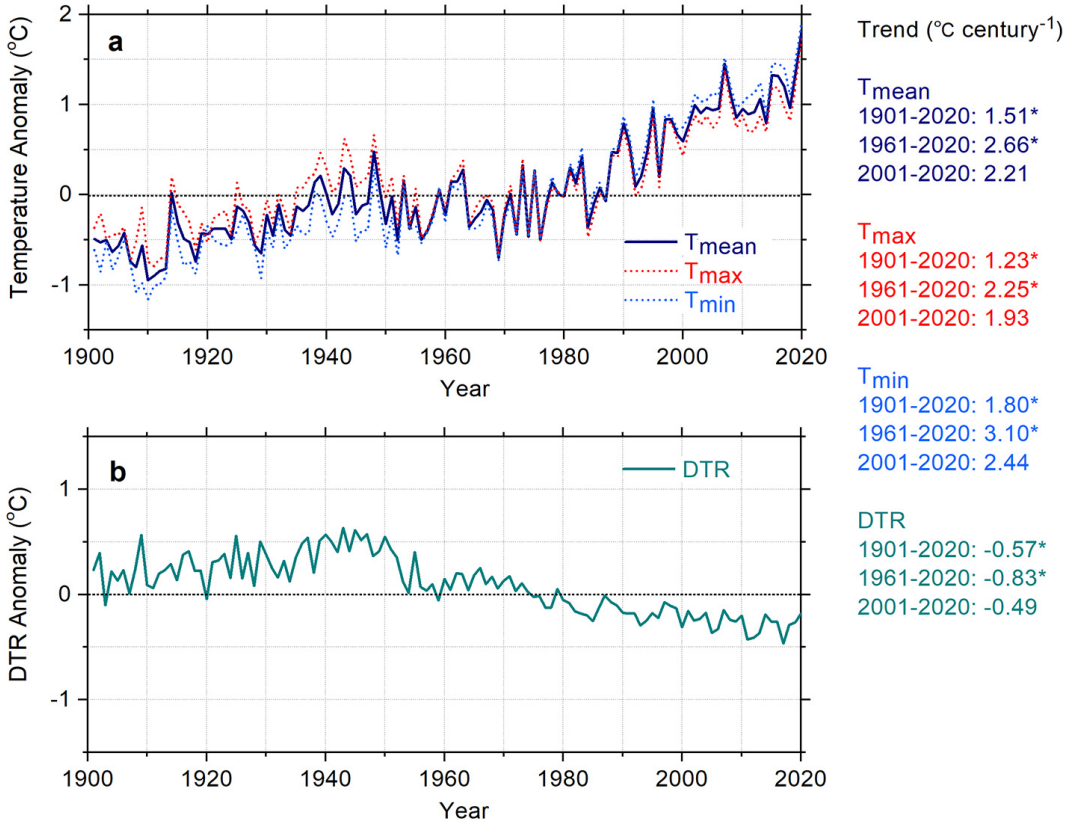

Fig. 2. Time series of (a) annual mean (T_{mean}), maximum (T_{max}), and minimum (T_{min}) temperature, and (b) diurnal temperature range (DTR) over Asia from 1901 to 2020 (anomalies relative to 1961–1990). Numbers to the right of the graphs: trend in different periods; *p ≤ 0.05

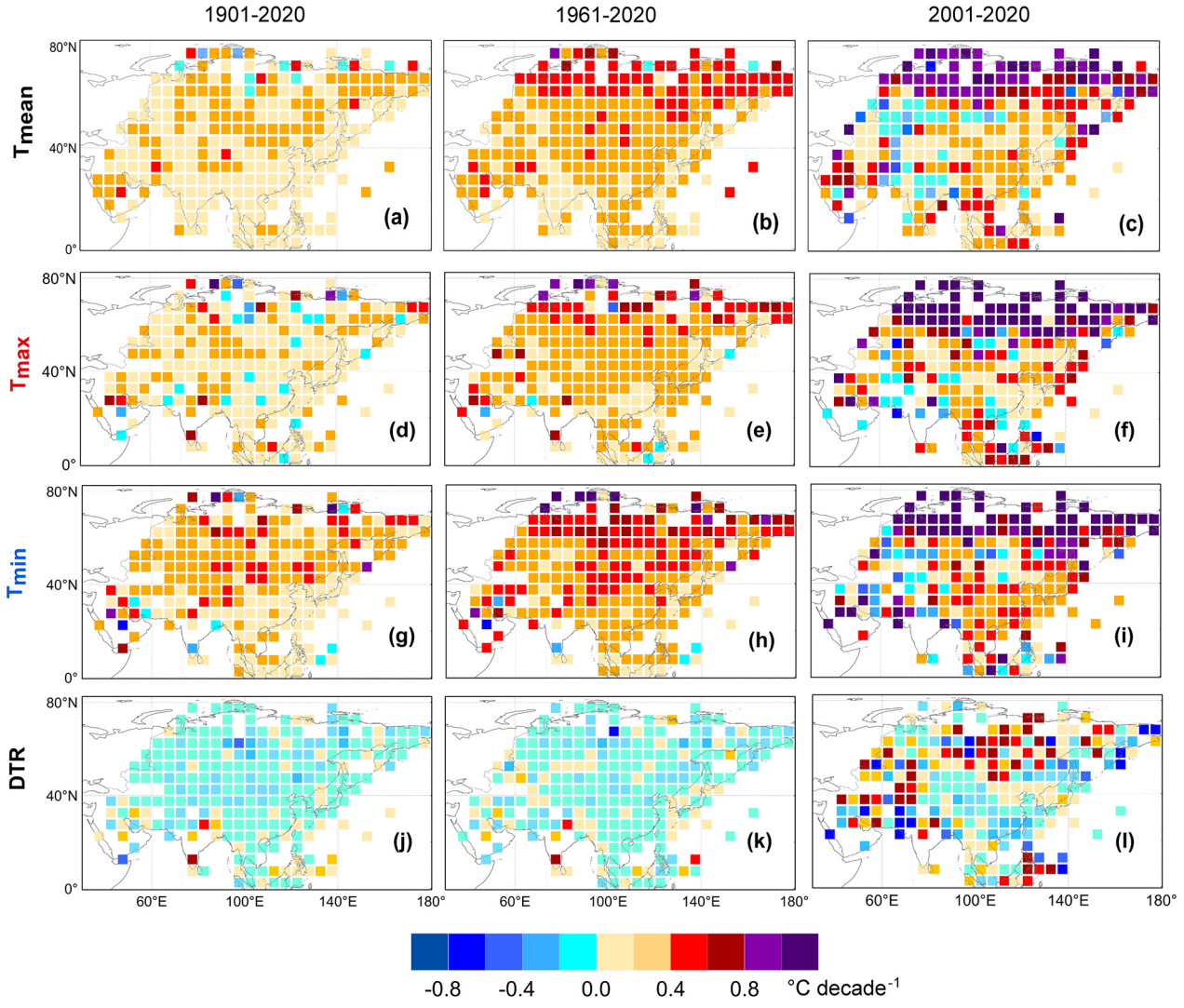

Fig. 3. Spatial distribution of the observed (a–c) T_{mean}, (d–f) T_{max}, (g–i) T_{min}, and (j–l) DTR trend over Asia in different periods (1901–2020, 1961–2020, and 2001–2020). Abbreviations as in Fig. 2

To further our understanding of Asian warming, we examined seasonal warming trends across Asia. Fig. 4 presents the seasonal trends in T_{mean}, T_{max}, T_{min}, and DTR from 1901 to 2020. Warming rates of T_{mean} in Asia during the cold seasons (spring and winter) are higher than those in the warm seasons (summer and autumn), and summer displayed the lowest warming rate of all seasons. T_{max} and T_{min} displayed non-symmetrical changes across seasons, contributing to the substantial DTR changes. The seasonal changes in DTR represent a more marked negative trend that occurs in the cold season (autumn and winter), especially in winter, as illustrated in Fig. 4d. During 1961–2020, Asian DTR shows a significant decreasing trend in the autumn and winter.

3.2. Asian warming at different latitudes

Furthermore, we investigated the differences between warming trends at different latitudes during different periods (Fig. 5). The warming of T_{min} is greater than T_{max} in the middle and high latitudes (>30° N). However, at low latitudes, the warming rate of T_{max} is greater than that of T_{min}, contributing to the long-term increase of DTR in these areas. However, this increase in DTR at lower latitudes is not statistically significant. Moreover, T_{max} and T_{min} at different latitudes exhibited asymmetric changes in different periods. Since 1901, DTR has shown a statistically significant decline at mid to high latitudes, with the most notable being high-latitude decline. Therefore, the decline of DTR at

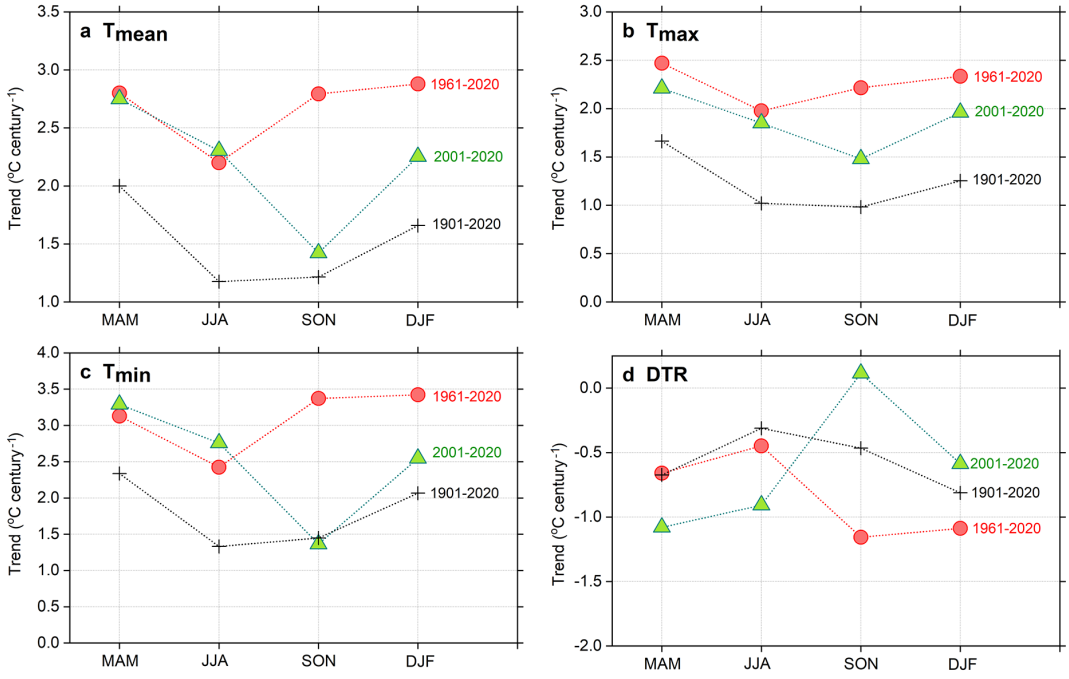

Fig. 4. Observed seasonal trend for (a) T_{mean}, (b) T_{max}, (c) T_{min}, and (d) DTR over Asia in different periods (1901–2020, 1961–2020, and 2001–2020). Abbreviations as in Fig. 2

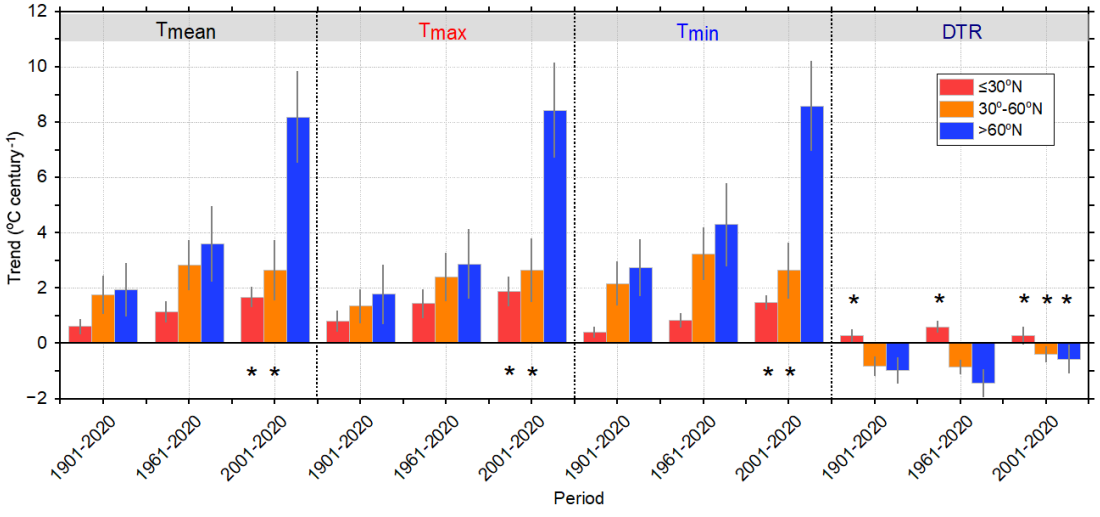

Fig. 5. Warming trend of T_{mean}, T_{max}, T_{min}, and DTR at different latitudes in different periods (1901–2020, 1961–2020, and 2001–2020). The distribution of stations at different latitudes and their long-term changes are shown in Fig. 1a,b. Error bars: ±1 SE. *p > 0.05. Abbreviations as in Fig. 2

mid and high latitudes has been identified as the primary driving factor for the overall DTR decline across Asia.

Additionally, the substantial high-latitude warming became more evident after 1961, and after 2001, this high-latitude warming became more significant. The series in Fig. 6 shows the contribution of high-latitude warming to the overall warming in Asia (difference between the entire Asian series and the mid-low latitude series) for T_{mean}, T_{max}, T_{min}, and DTR. The contribution of high-latitude warming gradually strengthened over time and had an increasingly substantial impact on Asian warming since the 2000s. After 2001, Asia's high-latitude warming trends are 3–4× more than those in middle and low latitudes (Fig. 3). Despite this, there is no significant change in the effect of high latitudes on the long-term DTR variation.

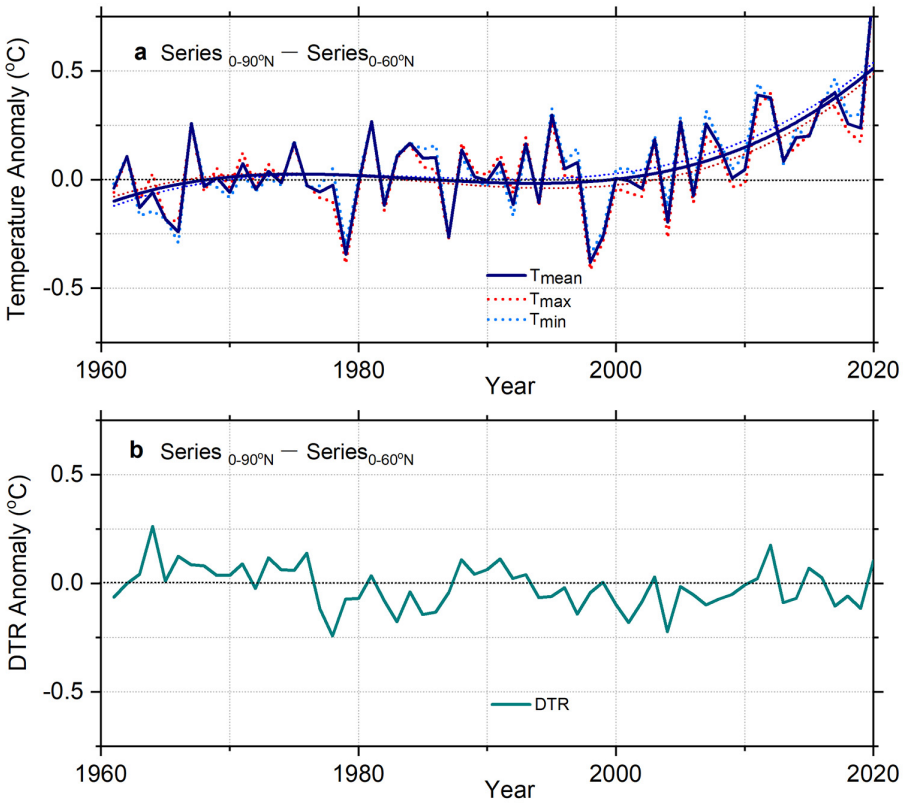

Fig. 6. Series showing contribution of high-latitude warming to the overall warming in Asia (difference between the entire Asian series and the mid-low latitude series, $Series_{0–90° N} – Series_{0–60° N}$) for (a) T_{mean}, T_{max}, and T_{min}, and (b) DTR. Smooth curves in (a): polynomial fitting curves for T_{mean}, T_{max}, and T_{min}, respectively. Abbreviations as in Fig. 2

3.3. Comparison of different data representations of warming in sub-regions of Asia

Fig. 7 compares the C-LSAT and CRU time series for Asian warming and the decadal means of the difference between the 2 series. It was found that the Asian warming represented by the C-LSAT and CRU series is generally consistent. The CRU series anomaly value is higher than the C-LSAT value before the 1960s; however, the difference between the 2 series gradually decreased after the 1960s. There is, however, a noticeable difference in the T_{min} represented by the 2 series in the early 20th century, which led to the CRU series representing much lower DTR values than the C-LSAT series before the 1960s.

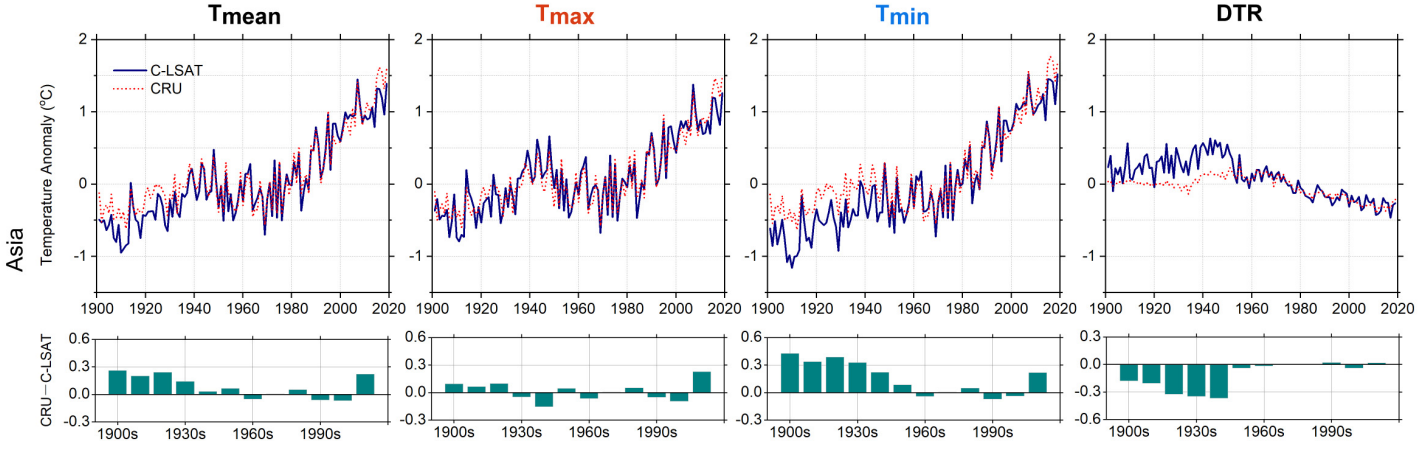

Fig. 7. Asian warming series based on C-LSAT and CRU data (upper row of graphs) for T_{mean}, T_{max}, T_{min}, and DTR, and the decadal means of the difference between the 2 types of series (lower row of graphs). Abbreviations as in Fig. 2

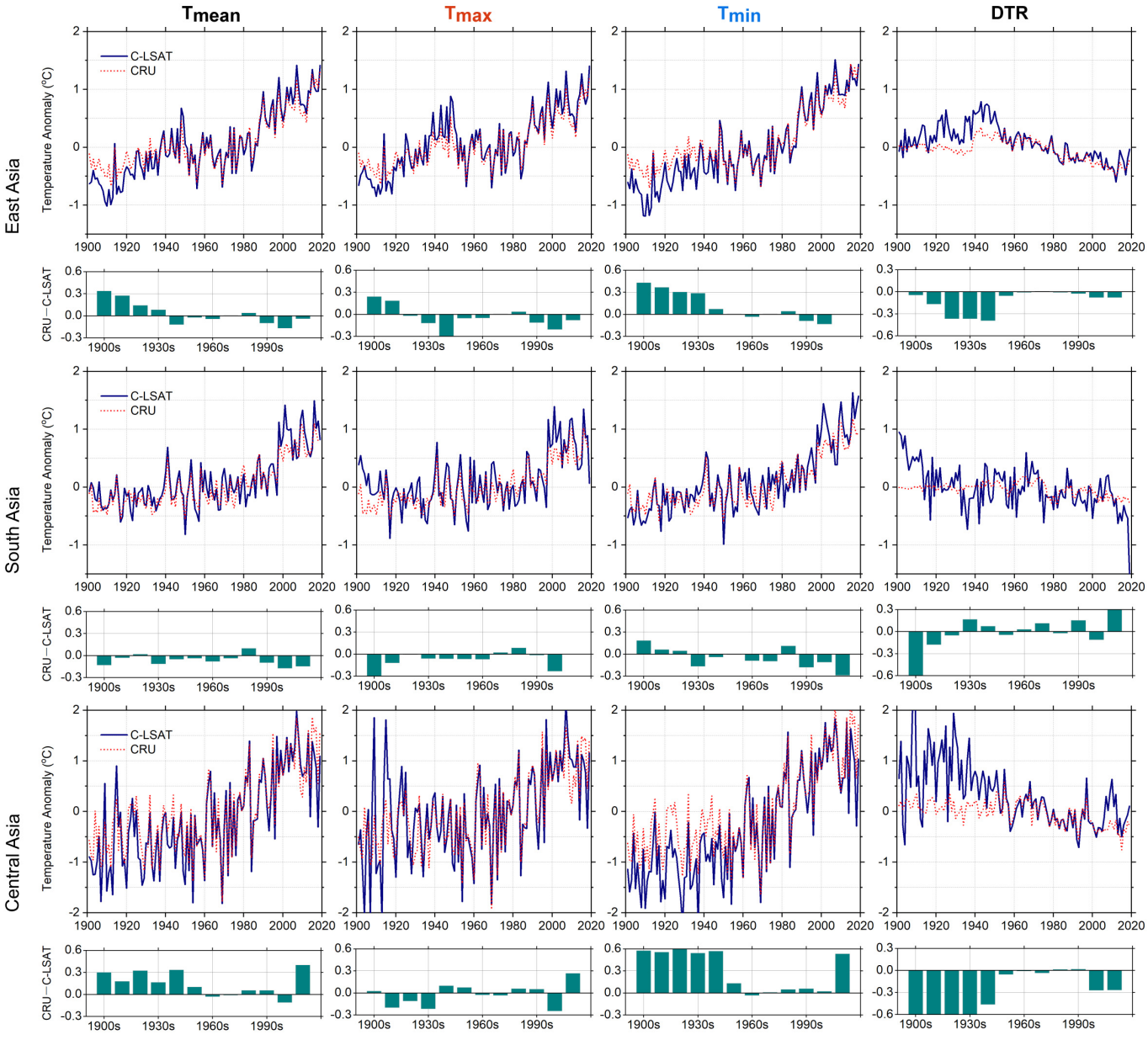

Fig. 8. As in Fig. 7 but for East Asia (upper rows), South Asia (middle rows), and Central Asia (lower rows)

Fig. 8 compares East, South, and Central Asia, similar to Fig. 7. In East Asia, the difference between CRU and C-LSAT was relatively small throughout the entire study period, and temperature changes showed a similar pattern to the warming of the entire Asian continent, with significant 3-stage changes. In contrast, the differences between CRU and C-LSAT in Central and South Asia are relatively large before the 1960s, especially in T_{min}. In addition, both series indicate no rapid warming period similar to Asia before the 1940s in Central and South Asia. Still, the most recent rapid warming period began in the 1960s, significantly earlier than in Asia.

Fig. 8 also reveals that both East and South Asian DTRs represented by CRU and C-LSAT both show a decreasing trend, and the DTR decline represented by C-LSAT is more substantial due to the lower T_{min} value of C-LSAT compared to CRU before the 1950s. In South Asia, the trend for DTR represented by CRU and C-LSAT both show insignificant changes, although there is a significant interannual variability difference between the 2 series. Overall, the warming characteristics represented by C-LSAT and CRU are similar in Asia and its sub-regions, but CRU exhibits weaker warming than C-LSAT.

4. ASIAN WARMING IN CMIP5/6 MODELS

Fig. 9a–d displays the observed and simulated time series of T_{mean}, T_{max}, T_{min}, and DTR. Overall, the CMIP5/6 multi-model ensemble (MME) can capture Asian warming from 1901 to 2020 (Fig. 9a–c); however, these models cannot simulate DTR interdecadal variability. Fig. 9e indicates that the trends simulated by the CMIP5/6 models for T_{mean}, T_{max}, and T_{min} are similar to the observed trends from 1901–2020 and the 1961–2020 period. The trends in the CMIP6 simulations for these parameters are larger than those in CMIP5. The DTR decline simulated by CMIP5/6 models is smaller than the observations, but CMIP6 is closer to the observations.

Based on the output data of the new-generation CMIP6 models, we also project future Asian warming. Fig. 10 illustrates T_{mean}, T_{max}, T_{min}, and DTR projected in CMIP6 models under SSP2-4.5 and SSP5-8.5, and the trends from 2021 to 2100. T_{mean}, T_{max},

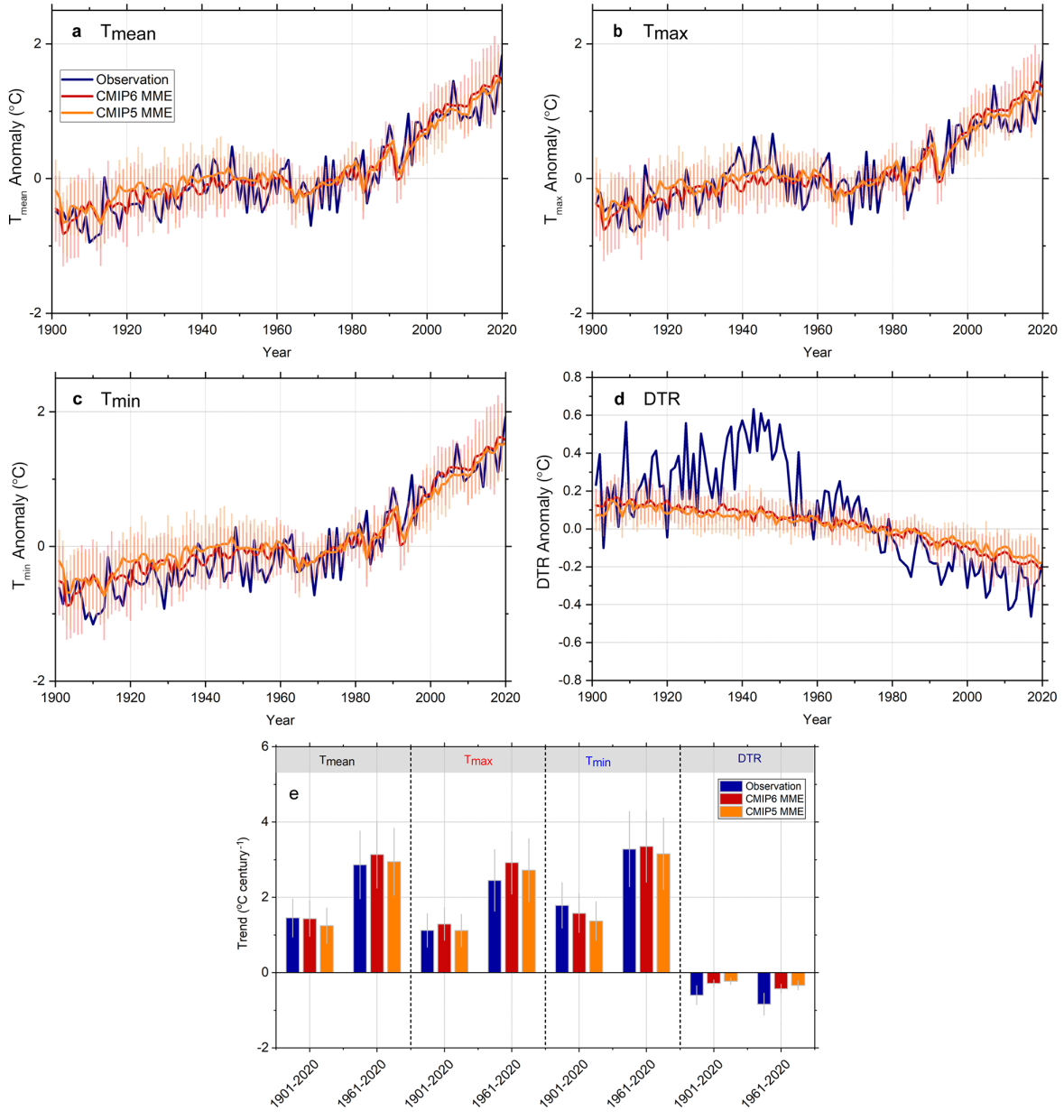

Fig. 9. Observed and CMIP5/6 simulated time series of historical (a) T_{mean}, (b) T_{max}, (c) T_{min}, and (d) DTR (anomalies relative to 1961–1990), and (e) warming trends for historical and future periods. Error bars in (a–d) on CMIP5/6 MME curves: ±1 SD; in (e): ±1 SE. Observation refers to observations from 1901 to 2020. Historical refers to the historical experiments in 11 (23) CMIP5 (CMIP6) models. MME: multi-model ensemble. Other abbreviations as in Fig. 2

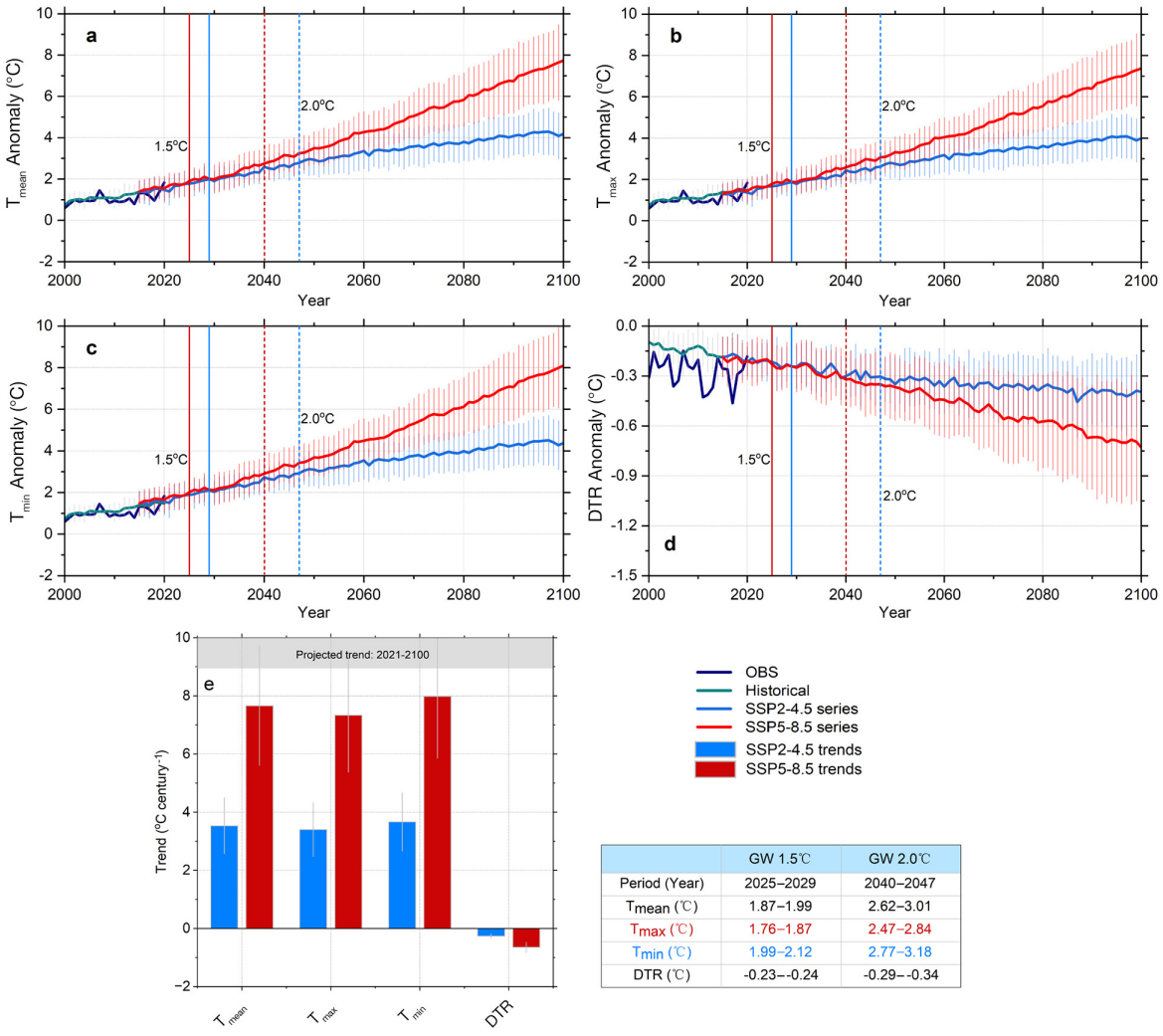

	GW 1.5℃	GW 2.0℃
Period (Year)	2025–2029	2040–2047
Tmean (℃)	1.87–1.99	2.62–3.01
Tmax (℃)	1.76–1.87	2.47–2.84
Tmin (℃)	1.99–2.12	2.77–3.18
DTR (℃)	-0.23–-0.24	-0.29–-0.34

Fig. 10. CMIP6 models-projected (a) T_{mean}, (b) T_{max}, (c) T_{min}, and (d) DTR (anomalies relative to 1961–1990) under SSP2-4.5 and SSP5-8.5, and (e) trends in 2021–2100. Error bars: ±1 SD. Vertical lines at global warming (GW) 1.5°C/2°C: the year when global-scale T_{mean} warming reaches 1.5°C/2°C relative to 1850–1900 (pre-industrial). Red and blue solid and dashed lines: years when GW 1.5 and 2°C, respectively, are reached under SSP5-8.5 and SSP2-4.5 scenarios. The table at the bottom represents the periods when global warming reaches 1.5 and 2°C under SSP2-4.5 and SSP5-8.5 scenarios, as well as the changes in various climate factors under the GW 1.5°C/2°C backgrounds.OBS: observation. Other abbreviations as in Fig. 2

and T_{min} is projected to continue to increase in Asia. Under the SSP2-4.5 scenario, Asia's T_{mean}, T_{max}, and T_{min} warming rates are 3.5, 3.4, and 3.7°C century^{-1}, respectively. The warming rate under the SSP5-8.5 scenario is about twice that of the SSP2-4.5 scenario or about 5–7× that of historical warming, implying unprecedented warming in Asia if SSP5-8.5 occurs. In the future, the projected warming rate of T_{min} in Asia is still higher than that of T_{max}, resulting in a continuous decline in DTR. Under the SSP5-8.5 scenario, the Asian DTR (–0.6°C century^{-1}) will continue to decline at a rate similar to the observed historical DTR decline. Under global warming of 1.5°C (2°C), T_{mean}, T_{max}, and T_{min} in Asia will increase by 1.87–1.99°C (2.62–3.01°C), 1.99–2.12°C (2.47–2.84°C), 1.99–2.12°C (2.77–3.18°C), respectively, compared with 1961–1990. This implies that the future warming in Asia will be much higher than the global level. The above results are similar to the conclusion reported by You et al. (2022) and Sun et al. (2019).

We also explored the warming rate in Asia at different latitudes. Table 2 lists projected T_{mean}, T_{max}, T_{min}, and DTR trends at different latitudes. The gradual increase in warming from low to high latitudes in Asia is projected to continue. The projected future warming rates at high latitudes are about 2× those at low latitudes. Overall, the CMIP6 models simulate accelerated warming mainly over high latitudes, suggesting that high-latitude regions are still particularly sensitive to future climate warming.

Table 2. Observed and projected mean (T_{mean}), maximum (T_{max}), and minimum (T_{min}) temperature, and diurnal temperature range (DTR) trends in Asia at different latitudes. The future projected trend is the multiple models mean in CMIP6. Underlined font: trend not significant

	Trend (°C century^{-1})			
	Observation (1901–2020)	CMIP6 simulation (1901–2020)	SSP 2-4.5 (2021–2100)	SSP 5-8.5 (2021–2100)
0–30° N				
T_{mean}	0.62	0.88	2.38	5.67
T_{max}	0.82	0.76	2.32	5.44
T_{min}	0.42	1.00	2.43	5.89
DTR	0.39	−0.24	−0.11	−0.44
30–60° N				
T_{mean}	1.76	1.47	3.43	8.01
T_{max}	1.35	1.32	3.32	7.71
T_{min}	2.18	1.62	3.55	8.32
DTR	−0.82	−0.30	−0.22	−0.61
60–90° N				
T_{mean}	1.95	2.27	4.99	10.95
T_{max}	1.78	2.11	4.77	10.41
T_{min}	2.75	2.44	5.21	11.49
DTR	−0.97	−0.33	−0.43	−1.08

5. DISCUSSION

5.1. Asian warming and its uncertainties

Based on observational data from the C-LSAT dataset, we analyzed the changes in the T_{mean}, T_{max}, T_{min}, and DTR over Asia from 1901 to 2020. The spatial coverage of early station records in Asia is relatively low (green squares in Fig. 1a), especially before the 1940s. This has resulted in significant uncertainty in the present results. We further investigated the influence of different station record lengths on Asian warming. Fig. 11 compares the time series of stations with observational records >100 yr and all stations, and the decadal mean of the differences between the 2 time series. Overall, the series of observational records >100 yr can represent the warming trend of Asia. One key distinction is that the long-term record station series demonstrates higher inter-annual variability when compared with the all-station series. Comparing different record-length series reveal relatively minor differences in T_{mean}. Compared with T_{mean}, the differences between T_{max} and T_{min} series from different record-length series are more pronounced, especially regarding their interannual variability. Compared with the T_{max} (T_{min}) series recorded at stations with >100 yr record, all stations feature lower anomalies in T_{max} (T_{min}) before the 1960s, with higher (lower) anomalies evident from the 1980s to the 1990s.

Table 3 compares global, Northern Hemisphere, and Asian warming trends since 1901. The results show that the Asian T_{mean} has increased by 1.56°C (1.3°C century^{-1}) since 1901, higher than the global and Northern Hemisphere warming rates. In particular, since 1961, the magnitude of Asian warming (2.9°C century^{-1}) has been greater than that of global warming (2.5°C century^{-1}). During 1998–2014, Asia showed a global warming slowdown of 1.1°C century^{-1}, similar to the global warming level since 1880. Table 3 also shows that the warming of T_{max} and T_{min} in Asia is also larger than that in the global case and the Northern Hemisphere since 1901. This also resulted in a more substantial DTR decline in Asia than globally and in the Northern Hemisphere.

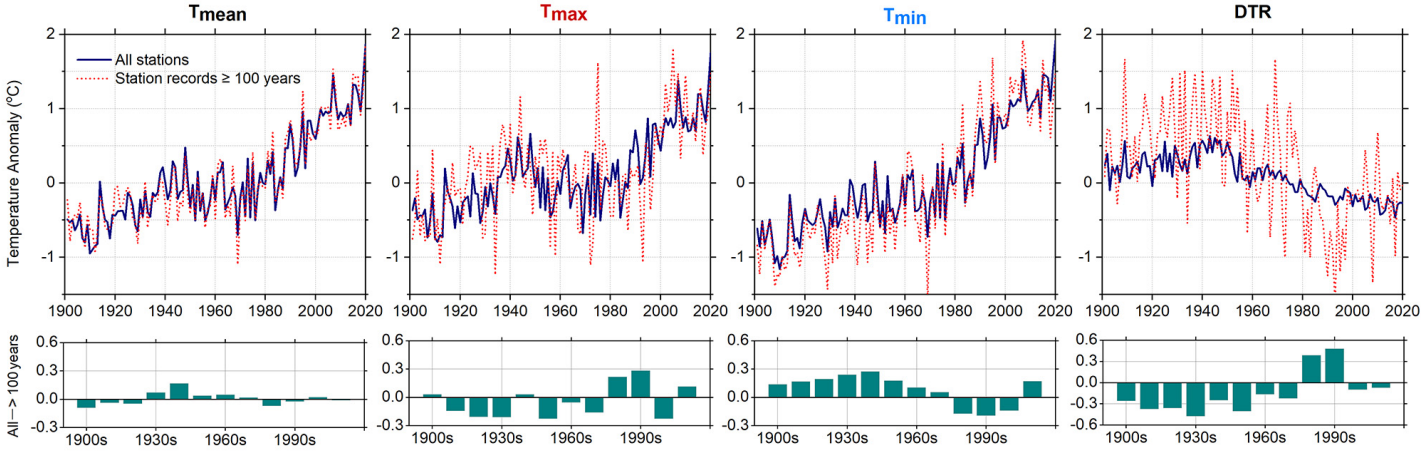

Fig. 11. Time series of stations with observational records >100 yr and all stations (upper row of graphs), and the decadal mean of the differences between the 2 time series (lower row of graphs)

Table 3. Comparison of warming rate in the global case, Northern Hemisphere, and Asia. Underlined font: trend not significant. Abbreviations as in Table 2

	Region	Data	Period	Trend (°C decade^{-1})	Reference
T_{mean}	Global	Multi-source data	1880–2020	0.11	IPCC (2021)
			1960–2020	0.25	
			1980–2020	0.30	
	Northern Hemisphere	C-LSAT	1901–2014	0.12	Sun et al. (2017), Xu et al. (2018)
			1979–2014	0.32	
			1998–2014	0.11	
	Asia	C-LSAT	1901–2020	0.15	This study
			1961–2020	0.27	
			2001–2020	0.22	
T_{max}/T_{min}/DTR	Global	C-LSAT	1901–2014	0.10 / 0.14 / −0.04	X. B. Sun et al. (2019)
			1951–2014	0.19 / 0.24 / −0.05	
			1979–2014	0.28 / 0.30 / −0.02	
			1998–2014	0.08 / 0.12 / −0.04	
	Northern Hemisphere	C-LSAT	1901–2014	0.11 / 0.15 / −0.04	X. B. Sun et al. (2019)
			1951–2014	0.20 / 0.26 / −0.05	
			1979–2014	0.31 / 0.35 / −0.02	
			1998–2014	0.09 / 0.12 / −0.05	
	Asia	C-LSAT	1901–2020	0.12 / 0.18 / −0.06	This study
			1961–2020	0.23 / 0.31 / −0.08	
			2001–2020	0.19 / 0.24 / −0.05	

5.2. Possible causes of Asian warming

Recently, studies have focused on the impact of greenhouse gases and anthropogenic aerosol emissions on Asian warming (Dong et al. 2016, Lu et al. 2022). Dong et al. (2016) indicated that the increase in greenhouse gas emissions was the main driver of warming in China and Northeast Asia. Tett et al. (2000) proposed that the increase in greenhouse gases and natural causes can explain the warming observed in the early 20th century. However, in the latter half of the 20th century, they found that the warming is mainly due to changes in greenhouse gas concentrations.

Our study confirmed that the mid-latitudes and high latitudes of Asia experience more substantial warming. However, studies have found that the causes of warming in the mid-latitudes and high latitudes of Asia are different. For the mid-latitude warming, Huang et al. (2013) and Guan et al. (2018) reviewed previous studies and indicated that the longwave radiation effect combined with strong land-atmosphere interaction amplified the warming in arid and semiarid regions. For the Arctic amplification phenomenon, this is generally believed to be caused by the radiative forcing of greenhouse gases in the atmosphere and the positive feedback from the melting ice and snow (Polyakov et al. 2012, IPCC 2021). The settlement of black carbon aerosols on the ice and snow surface could accelerate the melting and, thus, the positive feedback process (Hansen & Nazarenko 2004). Recent research has also emphasized the role of natural climate variability in Arctic warming amplification (e.g. Chylek et al. 2009, Lee 2012, Dai et al. 2019). It was also shown that the inter-decadal temperature variability in the polar areas was mainly related to the North Atlantic Oscillation (NAO).

Another primary reason for Asian warming that cannot be ignored is urbanization. On a global scale, urbanization may have little impact on the temperature trends estimated from the existing observational networks (Jones et al. 1990, 2008, Peterson & Owen 2005, Brohan et al. 2006). Zhang et al. (2021) also concluded that the impact of urbanization on global land surface air temperature is >12%, while the impact on regional scales, such as subcontinent-scale surface temperature trends in East Asia, is close to 25%. This is also similar to previous assessments of the contribution of urbanization to surface temperature trends in East Asia and China (Zhou et al. 2004, Hua et al. 2008, Ren & Zhou 2014). In East Asia,

urbanization influenced the surface air temperature trends obtained by the existing observational networks. It contributed >27% to the T_{mean} warming trends (0.25°C decade^{-1}) of mainland China's national reference climate and primary meteorological stations for nearly half a century (Zhang et al. 2010, Ren & Zhou 2014). This has become the primary source of uncertainty in mainland China's estimates of temperature changes (Ren et al. 2008, Zhang et al. 2010, Yang et al. 2011, Ren & Zhou 2014). The records of surface air temperature in Japan and the Korean Peninsula have been noticeably influenced by urbanization (Chung et al. 2004, Fujibe 2009), and also indicate that the effects of urbanization can be detected even at slightly urbanized sites in Japan (Fujibe 2009). Furthermore, Sun et al. (2021) found that urbanization contributed 25.9, 28.2, and 43.6% to T_{max}, T_{min}, and DTR trends in East Asia during 1951–2018, respectively. This indicates that DTR trends are more sensitive to the effects of urbanization. Therefore, it is necessary to evaluate the contribution of urbanization in the future.

This study found an increasing trend in DTR at low latitudes, but it is not statistically significant. Studies conducted by Easterling et al. (1997) and Thorne et al. (2016) both indicate an increasing trend in DTR at low latitudes in Asia, occurring specifically in India and Indonesia, since 1901. Kumar et al. (1994) investigated 121 observation stations in India and reported a statistically insignificant trend of an increase in DTR from 1901 to 1987. Their study also revealed that the effects of urbanization and altitude on DTR changes were negligible. Sen & Balling (2005) confirmed the insignificant trend of an increase in India's DTR from 1931 to 2002. Furthermore, their study found a significant negative correlation between Indian cloud cover and DTR, although the cloud cover trend was statistically insignificant. The above studies indicate that the long-term changes in cloud cover primarily explain the statistically insignificant trend of increase in low-latitude DTR. Therefore, the differential changes in DTR between high and low latitudes in Asia are primarily driven by the spatial heterogeneity of cloud cover changes.

6. CONCLUSIONS

Based on a newly developed observation dataset with 2658 stations and CMIP5/6 output data in Asia, we analyzed the changes in Asia's T_{mean}, T_{max}, T_{min}, and DTR during 1901–2100. The key findings and conclusions are as follows:

(1) Overall, the observed annual mean land surface air temperature over Asia has increased significantly since 1901, and T_{mean}, T_{max}, and T_{min} increased by 1.81, 1.47, and 2.15°C during 1901–2020, respectively. The T_{min} warming rate is about 1.5× that of T_{max}, resulting in a 0.68°C decrease in DTR. Asian warming represented by the C-LSAT and CRU series is generally consistent. The CRU series anomaly value is higher than the C-LSAT series anomaly value before the 1960s, and the difference between the 2 series gradually decreased after the 1960s. In addition, the warming rate of T_{min} is larger than that of T_{max}, especially in high latitudes, which directly leads to a long-term decreasing trend of DTR over Asia. Moreover, The temperature increase in Asia's cold season (winter and spring) is larger than in the warm season (summer and autumn).

(2) Regionally, Asia exhibits an overall warming trend with a gradual increase in spatial warming from low to high latitudes, and the effect of high-latitude warming has gradually strengthened since the 2000s. Moreover, both the CRU and C-LSAT series indicate that the warming in East Asia is similar to that of the entire Asian continent, with 2 rapid warming periods: before the 1940s and after the 1970s. The rapid warming in South Asia and Central Asia began in the 1960s, earlier than the rapid warming in East Asia that started in the 1970s. The warming characteristics represented by C-LSAT and CRU are similar in Asia and its sub-regions, but CRU exhibits weaker warming compared to C-LSAT.

(3) For the historical period (1901–2020), the multi-model ensemble in CMIP5/6 can capture overall Asian warming. The trends in T_{mean}, T_{max}, and T_{min} simulated by CMIP5/6 models are close to the observations during 1901–2020 and 1961–2020, but the trends in CMIP6 simulations are larger than those in CMIP5. The DTR decline simulated by CMIP5/6 models is lower than the observations, but CMIP6 is closer to the observations. In the future, the warming of T_{mean}, T_{max}, and T_{min} in Asia is projected to continue. Under the SSP2-4.5 scenario, the warming rate of T_{mean}, T_{max}, and T_{min} in Asia is increasing by 3.5, 3.4, and 3.7°C century^{-1}, respectively. The warming rate under the SSP5-8.5 scenario is about 2× that of the SSP2-4.5 scenario or about 5–7× that of historical warming. This implies that Asia will face unprecedented warming under the SSP5-8.5 scenario.

Acknowledgements. This study is supported by the National Key Research and Development Program of China (2018YFA0605603), the Natural Science Foundation of China (42005036), the Science and Technology Program of Guangzhou (202102021188), the development fund of the

South China Sea Institute of Oceanology of the Chinese Academy of Sciences (SCSIO202203), and the Independent Research Project Program of State Key Laboratory of Tropical Oceanography (LTOZZ2102). We thank the 3 anonymous reviewers for providing valuable suggestions. The CMIP6 model data can be downloaded from https://pcmdi.llnl.gov/CMIP6/. The observational data (CMA-LSAT dataset) can be obtained from the National Meteorological Information Center, China Meteorological Administration, http://data.cma.cn/.

LITERATURE CITED

Alcamo J, Dronin N, Endejan M, Golubev G, Kirilenko A (2007) A new assessment of climate change impacts on food production shortfalls and water availability in Russia. Glob Environ Change 17:429–444

Brohan P, Kennedy JJ, Harris I, Tett SFB, Jones PD (2006) Uncertainty estimates in regional and global observed temperature changes: a new dataset from 1850. J Geophys Res D Atmos 111:D12106

Cao LJ, Zhao P, Yan ZW, Jones P, Zhu Y, Yu Y, Tang G (2013) Instrumental temperature series in eastern and central China back to the nineteenth century. J Geophys Res D Atmos 118:8197–8207

Chen F, Huang W, Jin L, Chen JH, Wang JS (2011) Spatiotemporal precipitation variations in the arid Central Asia in the context of global warming. Sci China Earth Sci 54:1812–1821

Chung U, Choi J, Yun JI (2004) Urbanization effect on the observed change in mean monthly temperatures between 1951–1980 and 1971–2000 in Korea. Clim Change 66:127–136

Chylek P, Folland CK, Lesins G, Dubey MK, Wang M (2009) Arctic air temperature change amplification and the Atlantic Multidecadal Oscillation. Geophys Res Lett 36: 61–65

Dai A, Luo D, Song M, Liu J (2019) Arctic amplification is caused by sea-ice loss under increasing CO_2. Nat Commun 10:121

Dash SK, Jenamani RK, Kalsi SR, Panda SK (2007) Some evidence of climate change in twentieth-century India. Clim Change 85:299–321

Dhiman RC, Pahwa S, Dhillon GPS, Dash AP (2010) Climate change and threat of vector-borne diseases in India: Are we prepared? Parasitol Res 106:763–773

Ding YH, Dai XS (1994) Temperature variation in China during the last 100 years. Qixiang 20:19–26 (in Chinese)

Ding YH, Ren GY, Zhao ZC, Xu Y, Luo Y, Li Q, Zhang J (2007) Detection, causes and projection of climate change over China: an overview of recent progress. Adv Atmos Sci 24:954–971

Dong BW, Sutton RT, Chen W, Liu X, Lu R, Sun Y (2016) Abrupt summer warming and changes in temperature extremes over Northeast Asia since the mid-1990s: drivers and physical processes. Adv Atmos Sci 33:1005–1023

Easterling DR, Horton B, Jones PD, Peterson TC and others (1997) Maximum and minimum temperature trends for the globe. Science 277:364–367

Fan X, Duan QY, Shen C, Wu Y, Xing C (2020) Global surface air temperatures in CMIP6: historical performance and future changes. Environ Res Lett 15:104056

Fujibe F (2009) Detection of urban warming in recent temperature trends in Japan. Int J Climatol 29:1811–1822

Groisman PY, Blyakharchuk TA, Chernokulsky AV, Arzhanov MM and others (2013) Climate changes in Siberia. In: Groisman PY, Gutman G (eds) Regional environmental changes in Siberia and their global consequences. Springer, Dordrecht, p 57–109

Guan XD, Shi R, Kong XX, Liu JC and others (2018) An overview of researches on land-atmosphere interaction over semi-arid region under global changes. Adv Earth Sci 33:995–1004 (in Chinese)

Hansen J, Nazarenko L (2004) Soot climate forcing via snow and ice albedos. Proc Natl Acad Sci USA 101:423–428

Harris I, Osborn TJ, Jones PD, Lister D (2020) Version 4 of the cru ts monthly high-resolution gridded multivariate climate dataset. Sci Data 7:109

Hua LJ, Ma ZG, Guo WD (2008) The impact of urbanization on air temperature across China. Theor Appl Climatol 93:179–194

Huang JP, Ji MX, Liu YZ, Lei Z and others (2013) An overview of arid and semi-arid climate change. Adv Clim Change Res 9:9–14 (in Chinese)

IPCC (2021) Climate change 2021: the physical science basis. Contribution of Working Group I to the Sixth Assessment Report of the Intergovernmental Panel on Climate Change. Cambridge University Press, Cambridge. www.ipcc.ch/report/ar6/wg1/

Jiang D, Hu D, Tian Z, Lang X (2020) Differences between CMIP6 and CMIP5 models in simulating climate over China and the East Asian monsoon. Adv Atmos Sci 37: 1102–1118

Jones PD (1994) Hemispheric surface air temperature variations: a reanalysis and an update to 1993. J Clim 7: 1794–1802

Jones PD, Groisman PY, Coughlan M, Plummer N, Wang WC, Karl TR (1990) Assessment of urbanization effects in time series of surface air temperature over land. Nature 347:169–172

Jones PD, Lister DH, Li Q (2008) Urbanization effects in large-scale temperature records, with an emphasis on China. J Geophys Res D Atmos 113:D16122

Jung HS, Choi Y, Oh JH, Lim GH (2002) Recent trends in temperature and precipitation over South Korea. Int J Climatol 22:1327–1337

Kumar KR, Kumar KK, Pant GB (1994) Diurnal asymmetry of surface temperature trends over India. Geophys Res Lett 21:677–680

Kumar D, Kodra E, Ganguly AR (2014) Regional and seasonal intercomparison of CMIP3 and CMIP5 climate model ensembles for temperature and precipitation. Clim Dyn 43:2491–2518

Lawrimore JH, Menne MJ, Gleason BE, Williams CN, Wuertz DB, Vose RS, Rennie J (2011) An overview of the Global Historical Climatology Network monthly mean temperature dataset, version 3. J Geophys Res D Atmos 116:D19121

Lee S (2012) Testing of the Tropically Excited Arctic Warming Mechanism (TEAM) with traditional El Niño and La Niña. J Clim 25:4015–4022

Li QX, Dong WJ, Li W, Gao XR, Jones P, Kennedy J, Parker D (2010) Assessment of the uncertainties in temperature change in China during the last century. Sci Bull (Beijing) 55:1974–1982

Lu CH, Sun Y, Zhang X (2022) Anthropogenic influence on the diurnal temperature range since 1901. J Clim 35: 7183–7198

Meleshko VP, Kattsov VM, Mirvis VM, Govorkova VA, Pavlova TV (2008) Climate of Russia in the 21st century.

1. New evidence of anthropogenic climate change and the state of the art of its simulation. Russ Meteorol Hydrol 33:341–350
Menne MJ, Williams CN, Vose RS (2009) The U.S. Historical Climatology Network monthly temperature data, version 2. Bull Am Meteorol Soc 90:993–1007
Om KC, Ren GY, Jong SI, Li S, Kang-Chol O, Ryang CH, Zhang P (2019) Long-term change in surface air temperature over DPR Korea, 1918–2015. Theor Appl Climatol 138:363–372
Overpeck J, Hughen K, Hardy D, Bradley R and others (1997) Arctic environmental change of the last four centuries. Science 278:1251–1256
Peterson TC, Owen TW (2005) Urban heat island assessment: Metadata are important. J Clim 18:2637–2646
Piao S, Ciais P, Huang Y, Shen Z and others (2010) The impacts of climate change on water resources and agriculture in China. Nature 467:43–51
Polyakov IV, Walsh JE, Kwok R (2012) Recent changes of arctic multiyear sea ice coverage and the likely causes. Bull Am Meteorol Soc 93:145–151
Ren G, Zhou Y (2014) Urbanization effects on trends of extreme temperature indices of national stations over mainland China, 1961–2008. J Clim 27:2340–2360
Ren GY, Zhou YQ, Chu ZY, Zhou J, Zhang A, Guo J, Liu X (2008) Urbanization effects on observed surface air temperature trends in North China. J Clim 21:1333–1348
Saseendran SA, Singh KK, Rathore LS, Singh SV, Sinha SK (2000) Effects of climate change on rice production in the tropical humid climate of Kerala, India. Clim Change 44: 495–514
Sen PK (1968) Estimates of the regression coefficient based on Kendall's tau. J Am Stat Assoc 63:1379–1389
Sen RS, Balling RC (2005) Analysis of trends in maximum and minimum temperature, diurnal temperature range, and cloud cover over India. Geophys Res Lett 32: L12702
Shi Y, Shen Y, Kang E, Li D, Ding Y, Zhang G, Hu R (2007) Recent and future climate change in northwest China. Clim Change 80:379–393
Sorg A, Bolch T, Stoffel M, Solomina O, Beniston M (2012) Climate change impacts on glaciers and runoff in Tien Shan (Central Asia). Nat Clim Change 2:725–731
Sun XB, Ren GY, Xu WH, Li Q, Ren Y (2017) Global land-surface air temperature change based on the new CMA GSAT dataset. Sci Bull (Beijing) 62:236–238
Sun C, Jiang Z, Li W, Hou Q, Li L (2019) Changes in extreme temperature over China when global warming stabilized at 1.5 °C and 2.0 °C. Sci Rep 9:14982
Sun XB, Ren GY, You QL, Ren Y and others (2019) Global diurnal temperature range (DTR) changes since 1901. Clim Dyn 52:3343–3356
Sun XB, Wang CZ, Ren GY (2021) Changes of diurnal temperature range over East Asia from 1901 to 2018 and its relationship with precipitation. Clim Change 166:1–17
Tang GL, Ren GY (2005) Reanalysis of surface air temperature change of the past 100 years over China. Clim Environ Res 10:791–798 (in Chinese)
Tett S, Jones GS, Stott PA, Hill DC and others (2000) Estimation of natural and anthropogenic contributions to 20th century temperature change. J Geophys Res D Atmos 107(D16):4306
Thorne PW, Menne MJ, Williams CN, Rennie JJ and others (2016) Reassessing changes in diurnal temperature range: a new dataset and characterization of data biases. J Geophys Res D Atmos 121:5115–5137
Wang XL (2008a) Penalized maximal *F* test for detecting undocumented mean shift without trend change. J Atmos Ocean Technol 25:368–384
Wang XL (2008b) Accounting for autocorrelation in detecting mean shifts in climate data series using the penalized maximal *t* or *F* test. J Appl Meteorol Climatol 47: 2423–2444
Xu WH, Li QX, Yang S, Xu Y (2014) Overview of global monthly surface temperature data in the past century and preliminary integration. Adv Clim Change Res 5: 111–117
Xu WH, Li QX, Jones PD, Wang XL and others (2018) A new integrated and homogenized global monthly land surface air temperature dataset for the period since 1900. Clim Dyn 50:2513–2536
Yan ZW, Ding YH, Zhai PM, Song LC, Cao LJ, Li Z (2020) Reassessing climatic warming in China since 1900. J Meteor Res 34:243–251
Yang X, Hou Y, Chen B (2011) Observed surface warming induced by urbanization in east China. J Geophys Res D Atmos 116:D14113
You QL, Cai ZY, Wu FY, Jiang Z, Pepin N, Shen SSP (2021) Temperature dataset of CMIP6 models over China: evaluation, trend and uncertainty. Clim Dyn 57:17–35
You QL, Jiang ZH, Yue X, Guo W and others (2022) Recent frontiers of climate changes in East Asia at global warming of 1.5°C and 2°C. NPJ Clim Atmos Sci 5:80
Yue S, Hashino M (2003) Temperature trends in Japan: 1900–1996. Theor Appl Climatol 75:15–27
Zhang AY, Ren GY, Zhou JX, Chu ZY, Ren YY, Tang GL (2010) Urbanization effect on surface air temperature trends over China. Acta Meteorol Sin 68:957–966 (in Chinese)
Zhang HM, Huang B, Lawrimore JH, Menne MJ, Smith TM (2020) NOAA Global Surface Temperature Dataset (NOAAGlobalTemp), version 5. NOAA National Centers for Environmental Information, Asheville, NC
Zhang PF, Ren GY, Qin Y, Zhai Y and others (2021) Urbanization effect on estimate of global trends in mean and extreme air temperature. J Clim 34:1923–1945
Zhou L, Dickinson RE, Tian Y, Fang J and others (2004) Evidence for a significant urbanization effect on climate in China. Proc Natl Acad Sci USA 101:9540–9544
Zhu YY, Yang S (2020) Evaluation of CMIP6 for historical temperature and precipitation over the Tibetan Plateau and its comparison with CMIP5. Adv Clim Change Res 11:239–251

Editorial responsibility: Eduardo Zorita, Geesthacht, Germany
Reviewed by: X. Chen and 2 anonymous referees

Submitted: December 14, 2022
Accepted: June 26, 2023
Proofs received from author(s): August 31, 2023